International Journal for Parasitology: Drugs and Drug Resistance 7 (2017) 120–129

Contents lists available at ScienceDirect

International Journal for Parasitology: Drugs and Drug Resistance

journal homepage: www.elsevier.com/locate/ijpddr

Current opinion

4-Nitro styrylquinoline is an antimalarial inhibiting multiple stages of *Plasmodium falciparum* asexual life cycle

Bracken F. Roberts [a], Yongsheng Zheng [b], Jacob Cleaveland [b], Sukjun Lee [c], Eunyoung Lee [c], Lawrence Ayong [d], Yu Yuan [b, **], Debopam Chakrabarti [a, *]

[a] Division of Molecular Microbiology, Burnett School of Biomedical Sciences, College of Medicine, University of Central Florida, Orlando, FL, USA
[b] Department of Chemistry, University of Central Florida, Orlando, FL, USA
[c] Institut Pasteur Korea, Seongnam-si, Gyeonggi-do, South Korea
[d] Center Pasteur, Yaounde, Cameroon

ARTICLE INFO

Article history:
Received 18 December 2016
Received in revised form
13 February 2017
Accepted 15 February 2017
Available online 21 February 2017

Keywords:
Antimalarials
Antiplasmodials
Natural-product-like compounds
Styrylquinoline
Invasion inhibitor

ABSTRACT

Drugs against malaria are losing their effectiveness because of emerging drug resistance. This underscores the need for novel therapeutic options for malaria with mechanism of actions distinct from current antimalarials. To identify novel pharmacophores against malaria we have screened compounds containing structural features of natural products that are pharmacologically relevant. This screening has identified a 4-nitro styrylquinoline (SQ) compound with submicromolar antiplasmodial activity and excellent selectivity. SQ exhibits a cellular action distinct from current antimalarials, acting early on malaria parasite's intraerythrocytic life cycle including merozoite invasion. The compound is a fast-acting parasitocidal agent and also exhibits curative property in the rodent malaria model when administered orally. In this report, we describe the synthesis, preliminary structure-function analysis, and the parasite developmental stage specific action of the SQ scaffold.

1. Introduction

Malaria afflicts about half of the world's populations causing about 500,000 deaths annually (World Health Organization, 2016). It is of great concern that the drugs available for malaria therapy, including artemisinin, are rapidly becoming ineffective because of the widespread prevalence of drug resistant parasites (Greenwood, 1995; Rieckmann, 2006). Although artemisinin-based combination treatments (ACTs) have been effective in controlling the disease in many malaria endemic areas, the appearance of parasites resistant to artemisinin derivatives in wide areas of Southeast Asia, from South Vietnam to central Myanmar, emphasizes the fragility of available malaria treatment measures (Ashley et al., 2014; Cui, 2011). Therefore, there is an urgent need for new drugs directed against novel cellular targets, either for monotherapy or as a combination with other antimalarials that would result in an immediate intervention in the asexual life cycle.

Natural product (NP)-derived compounds are the richest source of novel pharmacophores as they are known to occupy biologically important chemical space (Cordier et al., 2008; Genis et al., 2012; Rishton, 2008; Vasilevich et al., 2012). NPs also have been pre-validated by nature, having gone through millions of years of natural selection to develop their ability to interact with biological macromolecules (Bon and Waldmann, 2010; Genis et al., 2012). Thus NPs exemplify unique structural elements that can be exploited as pre-validated starting points for novel synthetic libraries (Bon and Waldmann, 2010). Critical evaluations of known drugs and natural products have been used to identify drug/NP-based substructural motifs, termed as “BioCores” (Kombarov et al., 2010). To identify new antimalarial hits with novel mechanism of action, we have screened a collection of compounds that incorporates features of “BioCore” and known antimalarials. This screening effort has identified a 4-nitro styrylquinoline (SQ) as an antiplasmodial pharmacophore. In this report, we present the initial structure activity relationship based on this core structure, *in vivo* efficacy and stage specific activity.

Abbreviations: BINAP, 2,2′-bis(diphenylphosphino)-1,1′-binaphthyl; *p*-$TsNH_2$, *p*-toluenesulfonamide.

* Corresponding author.
** Corresponding author.
E-mail address: dchak@ucf.edu (D. Chakrabarti).

http://dx.doi.org/10.1016/j.ijpddr.2017.02.002

2. Materials and methods

2.1. P. falciparum culture and viability assay

P. falciparum Dd2 (chloroquine-resistant) and 3D7 (chloroquine-sensitive) were cultured in human A^+ erythrocytes using a modified Trager and Jensen (1976) method in RPMI 1640 medium with L-glutamine (Invitrogen) and supplemented with 25 mM HEPES, pH 7.4, 26 mM $NaHCO_3$, 2% dextrose, 15 mg/L hypoxanthine, 25 mg/L gentamycin, and 0.5% Albumax II. Cultures were maintained at 37 °C in 5% CO_2 and 95% air. Parasite viability was determined using a SYBR green I-based assay (Bennett et al., 2004; Johnson et al., 2007; Smilkstein et al., 2004). Different dilutions of the compound in DMSO were added to the *P. falciparum* culture at a 1% parasitemia and 2% hematocrit in 96-well plates (SantaCruz Biotechnology). Maximum DMSO concentration was less than 0.125%. Chloroquine at 1 μM was used as a positive control to determine the baseline value. Following 72 h incubation at 37 °C, the plates were frozen at −80 °C. Plates were thawed and 100 μL of lysis buffer (with 20 mM Tris-HCl, 0.08% saponin, 5 mM EDTA, 0.8% Triton X-100, and 0.01% SYBR Green I) was added to each well. Fluorescence emission from the plates was read using a Synergy H4 hybrid multimode plate reader (Biotek) set at 485 nM excitation and 530 nM emission after incubation in the dark for 30 min at 37 °C.

2.2. Library of compounds for screening

To select unique chemotypes we divided 50,000 BioCore (BioDesign) compounds (www.asinex.com) into clusters, using the cheminformatics software package Molsoft ICM Chemist Pro (www.molsoft.com/icm_pro.html) and JKlustor (ChemAxon). This analysis identified 2115 clusters. A central compound from each cluster was selected for purchase as this allowed us to maximize representation of the entire library set at minimal cost.

2.3. Cytotoxicity assay

Compounds at different dilutions were assessed for cytotoxicity in 384 well clear bottom plates (Santa Cruz Biotechnology) using HepG2 human hepatocyte cells at 2500 cells/well. The plates were incubated for 48 h at 37° C in an atmosphere containing 5% CO_2. Twenty μL MTS [(3-(4,5-dimethylthiazol-2-yl)-5-(3-carboxymethoxyphenyl)-2-(4-sulfophenyl)-2*H*-tetrazolium), CellTiter 96® Aqueous non-radioactive cell proliferation assay (Promega) reagent was added to each well and the plates were incubated for an additional 3 h. Cell viability was obtained by measuring the absorbance at 490 nm using Synergy H4 hybrid multimode plate reader (BioTek).

2.4. Physicochemical parameters

The aqueous solubility at pH 7.4 was assessed by UV−visible absorption based method (Avdeef, 2001). The permeability was evaluated by the *in vitro* double-sink parallel artificial membrane permeability assay (Kansy et al., 1998) that is a model for the passive transport from the gastrointestinal tract into the blood stream. The microsomal stability (Janiszewski et al., 2001) was determined by incubating the compound with mouse liver microsomes in the presence or absence of NADPH.

2.5. General chemistry

All chemicals and solvents were purchased from commercial vendors and used without further purification unless otherwise noted. Analytical TLC was performed with Silicycle silica gel 60 F254 plates; visualized by means of a UV light or spraying with chemical stains. Chromatography was performed with Silicycle silica gel (230–400 mesh) and using appropriate solvents as eluent. NMR spectra were recorded on a Bruker AV-400 or a Varian VNMRS 500 spectrometer. Proton chemical shifts were referenced relative to residual $CDCl_3$ proton signals at δ 7.27 ppm Data for ^1H NMR are reported as follows: chemical shift (ppm), multiplicity (s = singlet, d = doublet, t = triplet, q = quartet, brs = broad singlet, m = multiplet), coupling constants (Hz), integration. Mass spectra were recorded on an Agilent 6230 TOF LCMS instrument.

Compounds **2** and **3** were prepared according to the previous literature procedures (Thomas et al., 2010). Additional general chemistry procedures are presented as supplementary content.

2.6. β-Hematin formation assay

Compounds were tested for inhibition of β-hematin formation using the method described in Sandlin et al. (2011). Briefly, 100 μM (final concentration) of compound was added to 384 well flat bottom plates (SantaCruz Biotechnology) followed by the addition of 20 μL water, 7 μL of acetone and 5 μL of 348 μM Nonidet P-40. Twenty five μL of 228 μM hematin-DMSO suspension was added to each well and the plate was incubated at 37° C in a shaking incubator for 6 h β-hematin formation was analyzed using pyridine ferrochrome assay (Ncokazi and Egan, 2005). In essence, 5% v/v final concentration of pyridine from a solution consisting of water, 20% acetone, 200 mM HEPES and 50% pyridine was used and incubated under the same conditions as above for 10 min. Resulting pyridine-ferrochrome complex was measured at 405 nm using Biotek Synergy H1 multireader.

2.7. Cellular inhibition mechanisms

P. falciparum Dd2 cultures were synchronized by magnetic separation of schizonts (Ribaut et al., 2008), followed by sorbitol treatment (Lambros and Vanderberg, 1979). Synchronized cultures were treated at 6, 18, 30, 42 h post-invasion with UCF 501 at 5× EC_{50}, Giemsa-stained thin smears were prepared at 12 h time intervals, and microscopically evaluated to assess the block in intra-erythrocytic maturation. Samples were also collected at these time intervals fixed in a solution containing 0.04% glutaraldehyde in PBS, permeabilized with 0.25% Triton X-100, treated with RNAse (50 μg/ml) and stained with 10.24 μM YOYO-1 (Bouillon et al., 2013). Flow cytometry acquisition was performed in ThermoFisher Attune NxT at a voltage of 260 with excitation wavelength of 488 nM and an optical filter of 530/30.

The effect of UCF 501 on merozoite egress and invasion was also analyzed by an image-based assay described previously (Roberts et al., 2016). Briefly, synchronized *P. falciparum* HB3 (chloroquine-sensitive) at 1.5% hematocrit and 5% parasitemia was exposed to each of N-acetylglucosamine (GlcNAc), E-64, artemisinin and UCF 501 at 10 μM final concentration for 24 h. The culture was than stained with wheat germ agglutinin-Alexa Fluor 488 conjugate and Mitotracker Red CMXRos each at 1 nM final concentrations, and incubated at 37 °C for 20 min. The culture was next fixed in a solution containing 4% paraformaldehyde and 5 μg/ml DAPI (4′,6-diamidino-2-phenylindole). Five image fields were captured at three wavelengths (405 nM, DAPI; 488 nM, Alexa fluor; and 635 nM, Mitotracker deep red) using Operetta 2.0 automated imaging system (Perkin Elmer) from each assay well (384-well glass plate, Matrical) with a 40× high numerical aperture objective.

Table 1
Activities of antiplasmodial scaffold UCF 501. EC_{50} values (±SD) are derived from 3 independent experiments, each with 3 replicates. The Z′ factors of these assays were >0.8. *P. falciparum* Dd2, chloroquine resistant; 3D7, chloroquine sensitive.

ID	Name	Structure	EC_{50} Dd2 (μM)	EC_{50} 3D7 (μM)	EC_{50} HepG2 (μM)
UCF 501	4-Nitro styrylquinoline (NSQ)	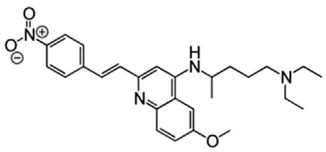	0.067 ± 0.008	0.119 ± 0.003	12.92 ± 0.07

2.8. In vivo efficacy determination

Standard variations of the Peters' four-day test (Peters, 1975; Sanni et al., 2002) with the compound following oral administration was used to test the *in vivo* efficacy in the murine malaria model using the *P. berghei* ANKA strain (Neill and Hunt, 1992). Female pathogen-free balb/c mice (8 weeks, ~25 g, 5 animals/group) were infected with 1×10^6 parasitized RBC (from a donor mouse) harboring *P. berghei* ANKA, by intraperitoneal (i.p.) injection. The animals were administered with the test compound by oral gavage (0.2 ml/dose), at 100 mg/kg twice daily for 4 consecutive days starting 6hr post-infection. Test compound UCF 501 was formulated in 0.5% hydroxyethylcellulose-0.1% Tween 80. The control group had only the vehicle. Thin blood smears were made from blood droplet from the temporal vein and Giemsa-stained for microscopic evaluation of parasitemia on day 4 and every day thereafter for 10 days and every other day beyond that. Mice were euthanized when parasitemia reached 40%. The animals were considered cured when smears were negative 30 days post infection. Elimination of existing infection was tested in Swiss Webster mice infected with 10^4 *P. berghei* ANKA expressing luciferase on day 0. Seventy two hours post infection mice were grouped (n = 5 per group) and received either vehicle (200 μL, 2% methylcellulose, 0.5% Tween80), chloroquine (200 μL, 40 mg/kg), or UCF 501 (200 μL, 100 mg/kg), via oral gavage once daily for 5 days at the Anti-Infectives Screening Core at New York Langone Medical Center, New York University (NYU). On day 7 post-infection, the mice were injected with 150 mg/kg of D-luciferin potassium salt substrate in

Table 2
Physicochemical properties of UCF 501. clogP is the calculated log octanol/water partition coefficient; F*sp3* is the fraction of *sp3* hybridized carbon atoms.

Property	UCF 501
Molecular Weight (g/mol)	462.6
clogP	3.76
Fsp3	0.37
Number of H Bond Donor	1
Number of N Atoms	4
Polar Surface Area (A^2)	83.2
Aqueous Solubility pH 7.4 (μg/mL)	289.7
Permeability pH 7.4 (−logPe)	2.9
Mouse Microsome Stability (% remaining at 60 min)	47.8
Microsomal stability $t_{1/2}$ (min)	56.2

Guidelines: Aqueous solubility: <10 μg/ml-low; 10–60 μg/ml-moderate; >60-high. Reference Permeability (−logPe) at pH 7.4: Verapamil-HCl 2.7; metoprolol- 3.6; rantidine- >5.9. Verapamil-HCl is considered highly permeable, metoprolol is moderately permeable; and rantidine is poorly permeable.

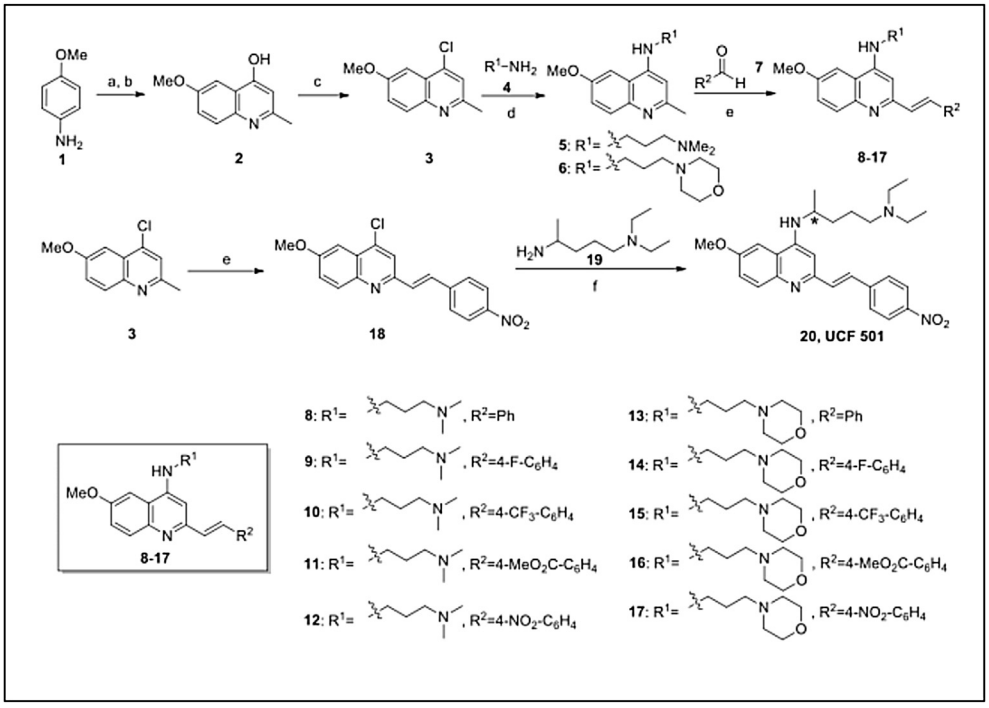

Fig. 1. Synthesis of compounds 1 to 20. (a) ethyl acetoacetate, $MgSO_4$, HOAc, EtOH, 90 °C; (b) Dowtherm, 270 °C; (c) $POCl_3$, reflux; (d) neat, pressure tube, 140 °C; (e) *m*-Xylene, *p*-$TsNH_2$,140 °C; (f) $Pd(OAc)_2$, BINAP, K_3PO_4, 1,4-dioxane, 85 °C. * symbol indicates chiral center.

Table 3
Structure activity relationship of SQ analogues. EC_{50} values (±SD) are derived from 3 independent experiments, each with 3 replicates.

Entry	SQ	Dd2 EC_{50} (μM)	3D7 EC_{50} (μM)	HepG2 EC_{50} (μM)
1	**8**	0.323 ± 0.04	0.302 ± 0.01	19.9 ± 0.04
2	**9**	0.137 ± 0.05	0.299 ± 0.04	12.6 ± 0.01
3	**10**	0.726 ± 0.04	0.605 ± 0.04	>20
4	**11**	0.138 ± 0.06	0.294 ± 0.06	14.9 ± 0.03
5	**12**	0.057 ± 0.03	0.197 ± 0.02	15.3 ± 0.05
6	**13**	0.303 ± 0.04	0.373 ± 0.03	18.0 ± 0.04
7	**14**	0.208 ± 0.04	0.310 ± 0.02	13.6 ± 0.05
8	**15**	0.735 ± 0.06	0.599 ± 0.03	>20
9	**16**	0.471 ± 0.08	0.322 ± 0.04	12.8 ± 0.02
10	**17**	0.123 ± 0.05	0.193 ± 0.05	15.7 ± 0.07
Chloroquine		0.172	0.011 ± 0.002	>20

Table 4
UCF 501 does not inhibit β-hematin formation. Chloroquine, a known inhibitor of β-hematin formation, along with 8-Hydroxyquinoline, a non-inhibitor, and UCF 501 were tested at a concentration of 100 μM for β-hematin formation inhibition using the NP-40 assay. These results are the average of two separate experiments. Compounds were tested at 100 μM.

Drug/compound	%Inhibition
Chloroquine	100 ± 1.78
8-Hydroxyquinoline	6 ± 0.42
UCF 501	0 ± 0.07

PBS, and imaged in an *in vivo* imaging system (IVIS, Lumina II, Perkin Elmer). The study was conducted using a protocol approved by the UCF and NYU institutional animal care and use committees (IACUC).

3. Results and discussion

3.1. Discovery of 4-nitro styrylquinoline (UCF 501) as selective antiplasmodial compound

To discover innovative antimalarial compounds that act on new cellular targets, we screened a library of 2115 compounds selected from the BioDesign and Biomimetic (also known as BioCore) platforms of the chemical compound vendor Asinex, which incorporates structural features of pharmacologically relevant natural products. We used an unbiased cell-based screen utilizing SYBR green I-based assay (Bennett et al., 2004; Johnson et al., 2007; Smilkstein et al., 2004) to identify antiplasmodial activities. For our primary screen, we used the chloroquine-resistant Dd2 strain and a stringent criterion of IC_{50} < 500 nM. We identified 39 unique scaffolds (1.8%) as initial hits based on the criterion. A 4-nitro styrylquinoline (SQ, UCF 501), exhibiting excellent antiplasmodial potency with an EC_{50} value of 67 nM (Table 1) was the most potent of these compounds. Furthermore, this chemotype exhibited better EC_{50} values for the chloroquine resistant Dd2 strain compared to the chloroquine sensitive 3D7 line, indicating that the compound may function differently from chloroquine. The EC_{50} for

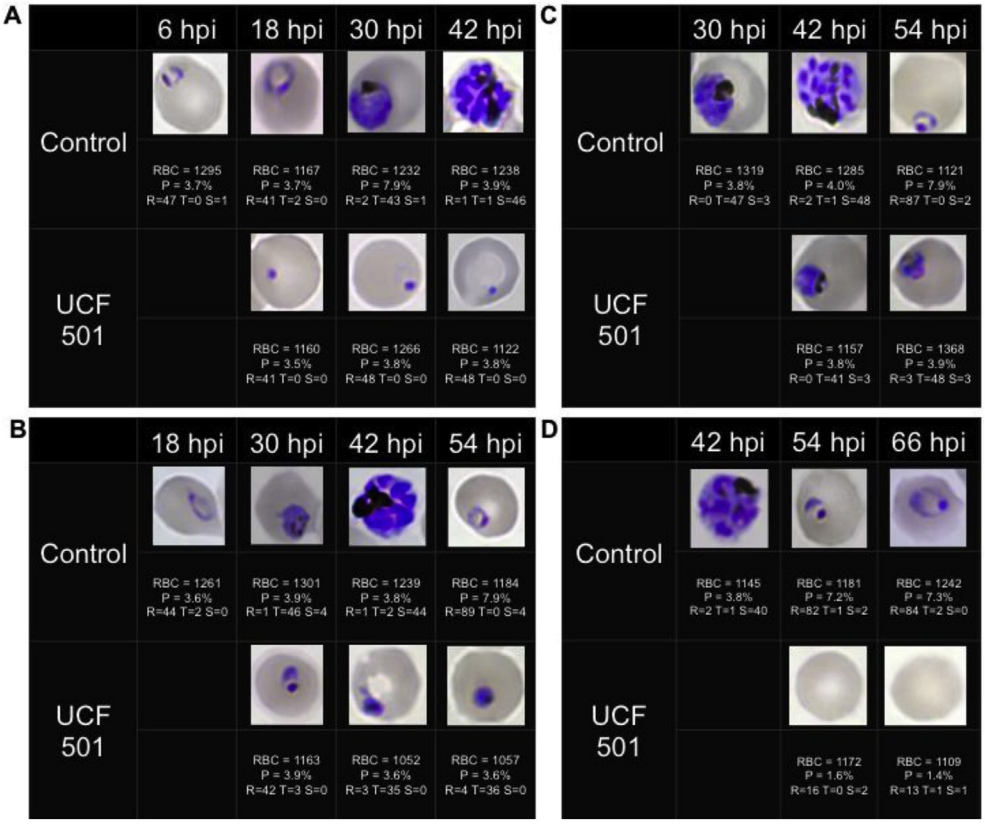

Fig. 2. UCF 501 blocks at multiple stages of intraerythrocytic development of *P. falciparum*. Tightly synchronized parasites were treated at (A) 6 h, (B) 18 h, (C) 30 h, and (D) 42 h post-invasion of merozoites with 5× EC_{50} concentration of the compound. Microscopic evaluation of Giemsa-stained-thin smears were done at 12 h intervals. Control represented infected red blood cells exposed to vehicle DMSO (0.1%). hpi, hours post invasion of red blood cells by merozoites. Representative figures from >80% of the infected RBCs are shown. Total number of observed RBCs, overall parasitemia (P) and the respective number of rings (R), Trophozoites (T), and Schizonts (S) are listed for each time point.

chloroquine is 15-fold higher in Dd2 (0.172 μM) compared to the 3D7 (0.011 μM) line. As a counter screen, we evaluated the cytotoxicity of these compounds in human hepatocyte cell line HepG2 using a MTS cell proliferation assay (Gupta et al., 2009). The EC_{50} value of UCF 501 in HepG2 cells was 12.9 μM demonstrating an excellent selectivity of 192 (Table 1).

3.2. Physicochemical properties and structure-activity relationship of UCF 501

We evaluated the compliance of UCF 501 with Lipinski's parameters. We also determined the *in vitro* physicochemical profiles (Avdeef, 2001) of UCF 501. As can be seen from the data presented in Table 2, the compound is in compliance with the Lipinski's

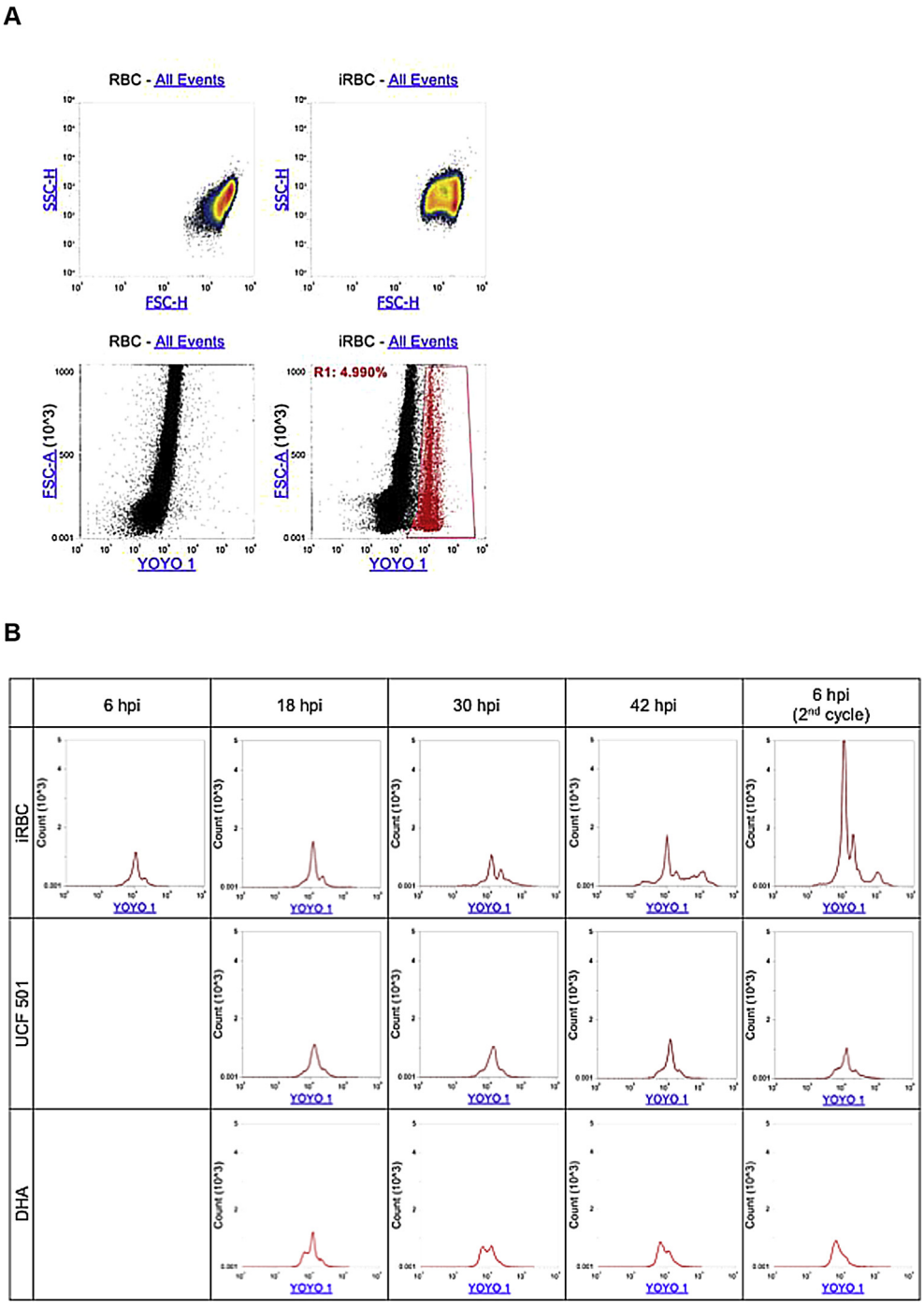

Fig. 3. UCF 501 Inhibits *Plasmodium falciparum* early in the intraerythrocytic cell cycle. Tightly synchronized cultures were treated with UCF 501, dihydroartemisinin (DHA), or vehicle at early ring stage (6 h post invasion) and then monitored every 12 h for a 48 h period. YOYO-1 treated samples were read on Attune NXT flow cytometer at a voltage of 260 with excitation wavelength of 488 nM and an optical filter of 530/30. Side scatter (SSC) log/Forward scatter (FSC) log density plots (A, top) and FSC log/YOYO-1 scatter plots (A, bottom) show distinct RBC and iRBC populations. (B) UCF 501 was added to tightly synchronized parasite cultures at A) 6 h, B) 18 h, C) 30 h, and D) 42 h post invasion and then incubated for at least 24 h. At 12-h increments treated cultures were fixed, permeabilized and stained with YOYO-1 for flow cytometry along with blood smears for Giemsa staining. Plots represent cell count in y-axis versus FL1 channel (488 nm Laser with 533/30 filter) representing DNA content. iRBC, infected red blood cells.

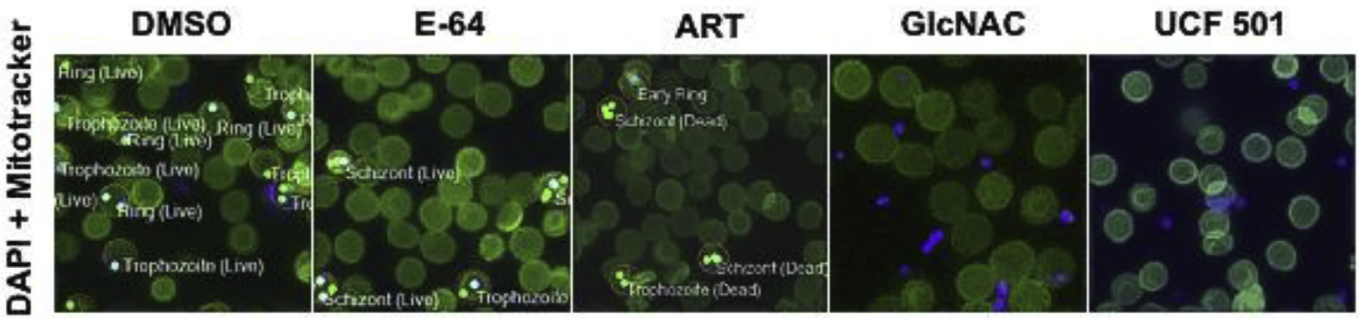

Fig. 4. Confocal plate micrograph showing parasite phenotype following 24 h compound exposure at 42 hpi (schizont stage). Sorbitol-synchronized cultures were treated at 1 μM concentration of UCF 501 or the reference compounds E-64 (protease inhibitor blocking egress), GlcNAc (N-acetylglucosamine, invasion inhibitor), or artemisinin at 42 hpi for 24 h. Cultures were then stained in a solution containing 1 nM each of wheat germ agglutinin-Alexa Fluor 488 conjugate and Mitotracker Red CMXRos followed by treatment with 4% paraformaldehyde and 5 μg/ml DAPI (2-(4-Amidinophenyl)-6-indolecarbamidine dihydrochloride, 4′,6-Diamidino-2-phenylindole dihydrochloride). Fluorescence imaging and automated detection of parasitized erythrocytes was done in an Operetta 2.0 system. Sample micrographs showing accumulation of extracellular merozoites in UCF 501 or GlcNAc-treated cultures compared to late rings ("Ring") in the solvent control wells, or schizonts in the E-64 and artemisinin-treated wells. The mitotracker-positive infected erythrocytes are indicated as "Live" whereas mitotracker-negative cells are labeled as "Dead".

parameters, and possesses good permeability and solubility. UCF 501 has a microsomal stability ($t_{1/2}$) close to 1 h, which is considered an acceptable value. It has been shown that compounds with similar microsomal stability are not expected to have significant *in vivo* clearance liabilities based on pharmacokinetic studies using 306 real world drug leads (Di et al., 2008).

The optimal physicochemical properties of UCF 501, in conjunction with its mouse microsomal stability profiles, make the SQ compound series an attractive platform for SAR studies. The preparation of arylvinylquinolines **8**–**17** and **20** are illustrated in Fig. 1. The key intermediate chloroquinoline **3** was synthesized from anisidine**1** and ethyl acetoacetate in 3 steps according to reported literature procedures (Thomas et al., 2010). The replacement of chloride by various amino groups was achieved by 2 different means. When an amino group is attached to the flanking end of the alkyl chain, a direct nucleophilic aromatic addition-elimination reaction (S_NAr) is able to convert **3** to the corresponding aminoquinoline (**5** or **6**) at elevated temperature (Gong et al., 2013); in contrast, when an amino group is attached to a secondary position such as **19**, a palladium catalyzed amination reaction proved to be more effective (Margolis et al., 2007). The addition of the styryl group, the *trans*-selective olefination reaction of 2-methylquinoline was accomplished by mixing desired aldehyde with quinoline in the presence of *p*-toluenesulfonamide and the reaction proceeded through an enamine intermediate (Yan et al., 2011).

In the work presented here we attempted to address two important questions. First of all, because the lead compound UCF 501 (**20**) has a chiral center (indicated by an asterisk symbol in Fig. 1) and its racemic form was used for the initial screening, SAR study of different amino groups at the quinoline 4 position will provide valuable information about the structural requirement for the antiplasmodial activity. Second, the potential cytotoxicity issue associated with the nitro group on the phenyl ring mandates a screening of the aromatic moiety in order to identify proper surrogate groups for future development. For these reasons, we have prepared SQs **8**–**17**, and their antiplasmodial activities are summarized in Table 3. We first replaced the chiral amine moiety in UCF 501 with 3- morpholinopropylamine and 3-dimethylaminopropylamine and compound **12** showed even better activity profiles compared to UCF 501, which indicated that a chiral center on the amino group alkyl chain was not necessary. The styryl group screening is focused on substitution of the aromatic group. When phenyl, 4-fluorophenyl, 4-trifluoromethylphenyl and 4-methoxycarbonylphenyl groups are incorporated into the quinoline core structure, the resulting SQ analogues all possess submicromolar activity against malaria parasites. Although nitro group analogues **12** and **17** are still the most potent compounds in each series, the EC_{50} values of 4-fluoro analogue **9** and 4-methoxycarbonyl analogue **11** are close to that of UCF 501, which makes them as good backup molecules if UCF 501 shows toxicity concerns in future development. Nitroaromatic compounds such as UCF 501 may be flagged as 'structural alert' because of potential toxicity issues (Walsh and Miwa, 2011). However, nitroaromatic drugs are in use to treat a wide variety of diseases, including parasitic diseases (Hemphill et al., 2006; Mattila and Larni, 1980; Pal et al., 2009; Raether and Hanel, 2003; Sorkin et al., 1985; Truong, 2009; Wilkinson et al., 2011).

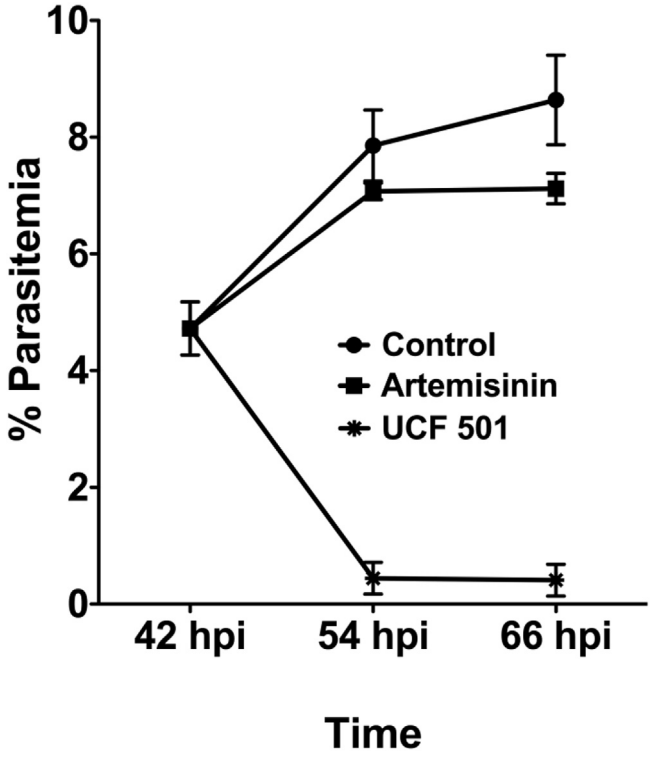

Fig. 5. Effect of UCF 501 on parasitemia when treated at the late schizont/segmenter stage. Cultures at 42 h post-invasion was exposed to UCF 501 or artemisinin at 5× EC_{50}.

3.3. UCF 501 does not inhibit β-hematin formation

Given the quinoline-based chemical structure of SQ, we assessed the inhibitory effect of UCF 501 on synthetic hemozoin (β-hematin) to rule out the possibility of hemozoin formation inhibition as seen with quinoline antimalarials such as, chloroquine and amodiaquine. We used a recently developed assay (Sandlin et al., 2011), which uses Nonidet P-40, a lipophilic detergent, as a surrogate for lipid-rich milieu of parasite's digestive vacuole. As evident from Table 4, while chloroquine, a known inhibitor of β−hematin formation, exhibited complete inhibition in this assay, UCF 501 is totally inactive. This result confirms that UCF 501, although a 4-aminoquinoline compound unlike chloroquine does not target hemozoin formation.

3.4. Stage specificity of UCF 501 growth inhibition

Next, we defined the developmental stage specific action of UCF 501 by both microscopy and flow cytometry. Precise delineation of the timing of action of an inhibitor provides valuable insight into the developmental growth and clinical clearance of the parasite. Recent flow cytometry-based analysis of twelve antimalarials, including ten that are widely used clinically, show that only artemisinin, artesunate, cycloheximide, and trichostatin A have significant effect on parasite's ring stage (Wilson et al., 2013). Furthermore, only artemisinin exhibited significant activity against schizonts, and none of the antimalarials prevented the invasion of merozoites (Wilson et al., 2013). Determination of stage-specificity also alludes to the mechanism of action of the UCF 501 and establishes if it is distinct from current antimalarials. To define the stage-specificities antiplasmodial action of UCF 501, we investigated its effects on the intraerythrocytic development of the parasite. Malaria parasite merozoites following invasion of erythrocytes matures through a series of developmental stages termed ring, trophozoite, schizont, and segmenter. Synchronized parasites were treated with 5× EC_{50} concentration at 6 (early ring), 18 (late ring/early trophozoite), 30 (early schizont), 42 (mature schizont/segmenters) hours post invasion of erythrocytes by merozoites and subsequently monitored at different post-invasion time-points (at 12 h intervals) for parasite cell cycle progression. As can be seen from Fig. 2, compared to the untreated cultures UCF 501 rapidly inhibited parasite's development from the early ring (Fig. 2A), late ring/trophozoite (Fig. 2B), and schizont stages (Fig. 2C). However, the compound was inactive in blocking merozoite egress as revealed by absence of schizonts in the treated cultures (Fig. 2D). When the culture was exposed to UCF 501 at 42 h post-invasion (hpi) ring-infected erythrocytes were scarcely seen compared to the untreated controls (Fig. 2D), suggesting a block in the invasion of merozoites. These findings on development stage specific action of UCF 501 were corroborated by flow cytometric analysis. The 6 hpi synchronized culture at the early ring stage was treated at 5× EC_{50} concentration, followed by withdrawal of aliquots at 12 h intervals to label the fixed parasite with YOYO-1 dye for flow cytometric assessment. As seen in Fig. 3, at 6 hpi (early ring) in the control culture the peaks represent singly, and multiple-infected cells based on DNA content. As the parasite matures, the DNA content increases and peaks start to spread because of schizogony. Following reinvasion parasitemia increases in the next growth cycle, which is represented by an increase in peak heights. At 54 hpi parasites are at the early ring stage of the next cycle, parasitemia is significantly higher, and three distinct peaks reappear. In contrast, exposure to UCF 501 and artemisinin at the ring stage (6 hpi) the maturation is blocked and as a result parasitemia does not increase. This suggests a block of intraerythrocytic maturation of parasite early in the developmental cycle when treated with UCF 501.

To further define the effects of UCF 501 on merozoite egress and invasion processes, we analyzed developmental maturation of parasite following exposure to UCF 501 using an image-based assay (Lee et al., 2014; Moon et al., 2013). As shown in Fig. 4, when the synchronized culture was exposed to UCF 501 at 42 hpi at the schizont stage, the DMSO (vehicle) treated culture showed rings inside RBC after 24 h of growth. The artemisinin treated culture had similar effect as the drug has no effect on invasion. E-64 (L-trans-epoxysuccinyl-leucylamido-(4-guanidino)butane, a cysteine protease inhibitor, completely blocks egress as shown by the presence of schizonts. In contrast, both N-acetylglucosamine (GlcNAc) and UCF 501 blocks invasion as evidenced by the presence of extracellular merozoites and absence of intracellular rings. N-

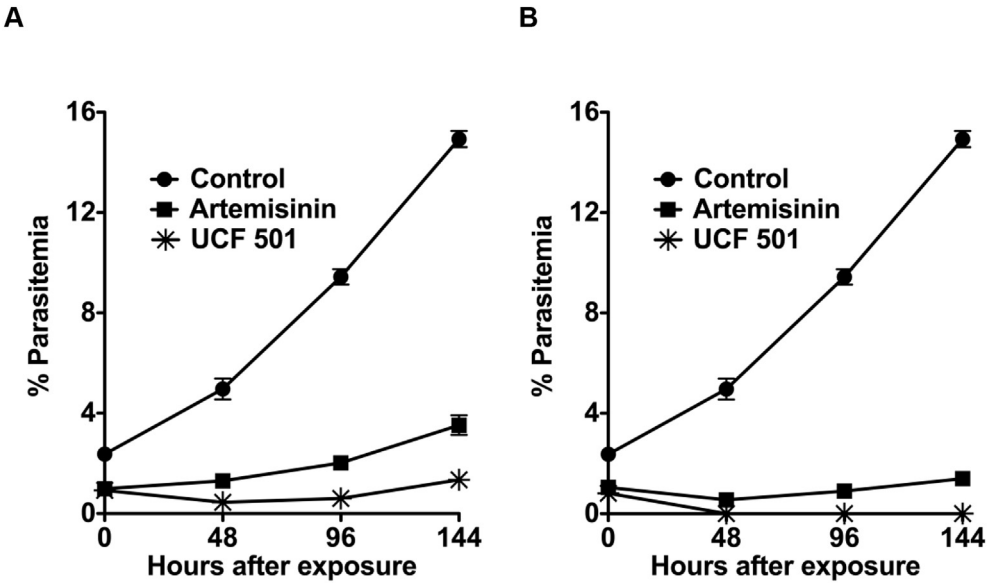

Fig. 6. UCF 501 is parasitocidal. Asynchronous cultures were exposed to 3× EC_{50} of UCF 501 (200 nM) or artemisinin (45 nM) for (A) 6 h, and (B) 12 h followed by washing and growing in the absence of the inhibitors.

acetylglucosamine is a reference invasion inhibitor (Howard and Miller, 1981).

To confirm the effect of UCF 501 on merozoite invasion of new cells, we quantified the parasitemia following treatment with the compound at the 42 h post-invasion time point for 24 h. As can be seen from Fig. 5, there is a significant reduction in culture parasitemia upon exposure to UCF 501 at 42 hpi compared to control cultures. In contrast artemisinin, which has no influence on merozoite invasion, does not cause similar marked reduction. These data suggest that UCF 501 has a significant effect on the merozoite viability and/or host cell invasion process. Collectively, the above data suggest that the molecular targets of the compound are likely to be essential for the merozoite survival and invasion processes, and for the early ring to the mid-trophozoite developmental stage. Further mechanistic characterization of the stage specific effect of UCF 501 will be the focus of future studies. These results underscore the novelty of the mechanism of action UCF 501 as it is distinct from current antimalarials which target either (a) the food vacuole of late-ring and trophozoite stage parasites, (b) the biosynthesis of folic acid in trophozoites (c) mitochondrion electron transport or (d) apicoplast translation (Dahl and Rosenthal, 2007; Famin and Ginsburg, 2002; Goodman et al., 2007; Krishna et al., 2004; Loria et al., 1999; Srivastava et al., 1997; Wilson et al., 2013).

3.5. UCF 501 is a fast-acting parasitocidal compound

Next, we assessed parasitocidal or parasitostatic properties of UCF 501, and if it is parasitocidal, then what would be the optimum time to achieve the 100% parasitocidal effect. Growing asynchronous parasites were exposed to 3× EC_{50} concentration of UCF 501 (200 nM) and artemisinin (45 nM) for 6, 12, 24 and 48 h followed by washing to remove the inhibitor and continue monitoring growth for 144 h. Parasitemia decreased significantly for both UCF 501 and artemisinin following 6 h exposure, although UCF 501 was more effective. Viable parasites showed signs of growth after 96 h following removal of drug (Fig. 6A). However, 12 h (Fig. 6B) or longer exposure (not shown) to UCF 501 resulted in complete loss of viability. In contrast, we observed that a total loss of viability could only be achieved with artemisinin at 3× EC_{50} concentration after 72 h of drug exposure (data not shown). Similar time course of artemisinin action has been reported earlier (Alin and Bjorkman, 1994). Furthermore, there was no sign of parasite recovery observed for up to one week. The results described above establish that UCF 501 is a fast-acting parasitocidal agent.

3.6. UCF 501 cures malaria in the rodent model

Because of excellent *in vitro* activity and novel stage-specific action of UCF 501, we evaluated the potential of this scaffold to cure malaria using the rodent malaria model. We used the *P. berghei* ANKA strain for infecting Balb/c mice as this strain produces histopathological and immunopathological features that are strikingly similar to human cerebral malaria (Neill and Hunt, 1992). As can be seen from Fig. 7A, UCF 501 cured malaria infection in mice when exposed to 100 mg/kg twice daily by oral administration in 4/5 mice in a standard Peters' four-day test (Peters, 1975; Sanni et al., 2002) when infection was initiated with 1 × 10^6 *P. berghei* ANKA cells, and the treatment was initiated 4 h post-infection. All four surviving mice did not show any evidence of infection up to day 30 and the parasitemia in one animal was 0.2% on day 22 and reached 40% on day 27, when it was euthanized. To assess the ability of UCF 501 to eliminate an established infection, treatment of animals was initiated 72 h post-infection. As can be seen from Fig. 7B, the delayed treatment almost cleared luciferase expressing parasite burden at 100 mg/kg once daily dose. Cure of malaria in the rodent

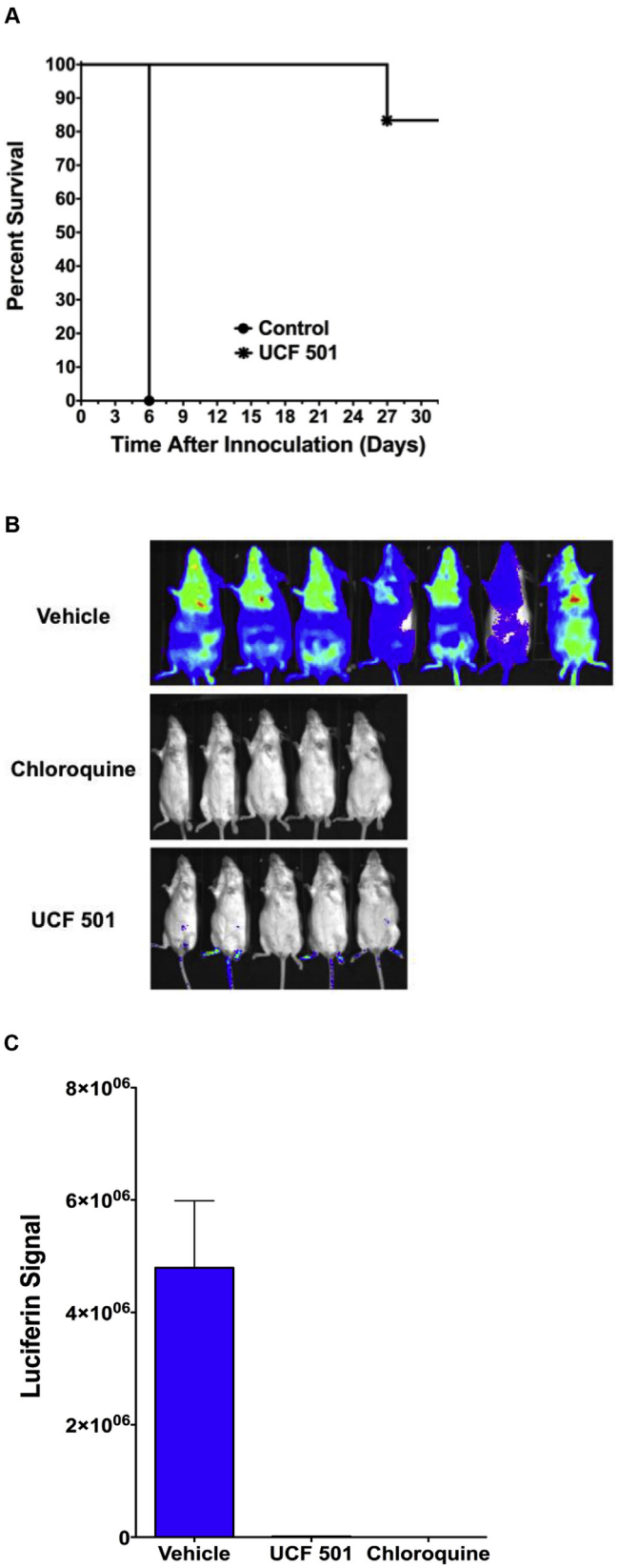

Fig. 7. UCF 501 exhibits curative property. (A) Effect of UCF 501 on the survivability of *P. berghei* ANKA infected Balb/c mice was evaluated. Mice were treated orally with UCF 501 twice daily at 100 mg/kg at the time of infection. (B & C) Swiss Webster mice were infected with *P. berghei* ANKA expressing luciferase, treated with 100 mg/kg orally once daily 72 h post-infection, and the luciferin signal was detected (B) and quantified (C) with an *in vivo* imaging system (IVIS).

model by UCF 501 is very significant because the *P. berghei* model is quite challenging, as it requires complete elimination of parasites, otherwise fatal parasitemia would recrudesce (Nallan et al., 2005). It is expected that with future optimization of SQ scaffold much improved *in vivo* efficacy could be achieved.

4. Conclusion

In spite of widespread resistance to 4-aminoquinolines (4-AQ) compounds, quinoline scaffold is still considered useful for the development of new generation of antimalarials and many attractive 4-AQ analogs have been synthesized recently (Saenz et al., 2012; Singh et al., 2009; Sinha et al., 2014; Tukulula et al., 2013). Although these newer generation of AQ analogs do not exhibit cross-resistance to chloroquine, it is unknown if their mechanisms of action are distinct from that of chloroquine. Many of these new AQ analogs are either known to inhibit β-hematin formation with IC_{50} in the submicromolar range, or their interaction with β-hematin is as yet unpublished. In that respect the absence of β-hematin inhibitory activity of UCF 501 is noteworthy. Furthermore, UCF 501, acts quickly (phenotypically observable developmental changes within 12 h of treatment) at all stages of the intraerythrocytic lifecycle. It is significant that UCF 501 inhibits merozoite invasion unlike any other approved drugs for malaria. This novel cellular action provides strong evidence that the SQ chemotype potentially is a new therapeutic option for malaria directed against unique cellular targets. Future isobologram analysis with lead compounds will define the utility of the SQ chemotype in combination therapies. In summary, our results suggest that SQ analogs in its ability to block all stages of parasite intraerythrocytic development, and rapidly clear parasites have immense potential as an antimalarial pharmacophore.

Acknowledgements

This work was supported by Burnett School of Biomedical Sciences Director's Impact Award, UCF College of Medicine research development intramural award, and NIH/NIAID AI117298. We thank Robert Banks at the UCF Animal Care Facility for his assistance and training with the BALB/c mice experiments. We also thank Ana Rodriguez at NYULMC for the IVIS imaging experiment.

Appendix A. Supplementary data

Supplementary data related to this article can be found at http://dx.doi.org/10.1016/j.ijpddr.2017.02.002.

References

Alin, M.H., Bjorkman, A., 1994. Concentration and time dependency of artemisinin efficacy against *Plasmodium falciparum* in vitro. Am. J. Trop. Med. Hyg. 50, 771–776.

Ashley, E.A., Dhorda, M., Fairhurst, R.M., Amaratunga, C., Lim, P., Suon, S., Sreng, S., Anderson, J.M., Mao, S., Sam, B., Sopha, C., Chuor, C.M., Nguon, C., Sovannaroth, S., Pukrittayakamee, S., Jittamala, P., Chotivanich, K., Chutasmit, K., Suchatsoonthorn, C., Runcharoen, R., Hien, T.T., Thuy-Nhien, N.T., Thanh, N.V., Phu, N.H., Htut, Y., Han, K.T., Aye, K.H., Mokuolu, O.A., Olaosebikan, R.R., Folaranmi, O.O., Mayxay, M., Khanthavong, M., Hongvanthong, B., Newton, P.N., Onyamboko, M.A., Fanello, C.I., Tshefu, A.K., Mishra, N., Valecha, N., Phyo, A.P., Nosten, F., Yi, P., Tripura, R., Borrmann, S., Bashraheil, M., Peshu, J., Faiz, M.A., Ghose, A., Hossain, M.A., Samad, R., Rahman, M.R., Hasan, M.M., Islam, A., Miotto, O., Amato, R., MacInnis, B., Stalker, J., Kwiatkowski, D.P., Bozdech, Z., Jeeyapant, A., Cheah, P.Y., Sakulthaew, T., Chalk, J., Intharabut, B., Silamut, K., Lee, S.J., Vihokhern, B., Kunasol, C., Imwong, M., Tarning, J., Taylor, W.J., Yeung, S., Woodrow, C.J., Flegg, J.A., Das, D., Smith, J., Venkatesan, M., Plowe, C.V., Stepniewska, K., Guerin, P.J., Dondorp, A.M., Day, N.P., White, N.J., Tracking Resistance to Artemisinin, C., 2014. Spread of artemisinin resistance in *Plasmodium falciparum* malaria. N. Engl. J. Med. 371, 411–423.

Avdeef, A., 2001. Physicochemical profiling (solubility, permeability and charge state). Curr. Top. Med. Chem. 1, 277–351.

Bennett, T.N., Paguio, M., Gligorijevic, B., Seudieu, C., Kosar, A.D., Davidson, E., Roepe, P.D., 2004. Novel, rapid, and inexpensive cell-based quantification of antimalarial drug efficacy. Antimicrob. Agents Chemother. 48, 1807–1810.

Bon, R.S., Waldmann, H., 2010. Bioactivity-guided navigation of chemical space. Acc. Chem. Res. 43, 1103–1114.

Bouillon, A., Gorgette, O., Mercereau-Puijalon, O., Barale, J.C., 2013. Screening and evaluation of inhibitors of *Plasmodium falciparum* merozoite egress and invasion using cytometry. Methods Mol. Biol. 923, 523–534.

Cordier, C., Morton, D., Murrison, S., Nelson, A., O'Leary-Steele, C., 2008. Natural products as an inspiration in the diversity-oriented synthesis of bioactive compound libraries. Nat. Product. Rep. 25, 719–737.

Cui, W., 2011. WHO urges the phasing out of artemisinin based monotherapy for malaria to reduce resistance. BMJ 342, d2793.

Dahl, E.L., Rosenthal, P.J., 2007. Multiple antibiotics exert delayed effects against the *Plasmodium falciparum* apicoplast. Antimicrob. Agents Chemother. 51, 3485–3490.

Di, L., Kerns, E.H., Ma, X.J., Huang, Y., Carter, G.T., 2008. Applications of high throughput microsomal stability assay in drug discovery. Comb. Chem. High Throughput Screen. 11, 469–476.

Famin, O., Ginsburg, H., 2002. Differential effects of 4-aminoquinoline-containing antimalarial drugs on hemoglobin digestion in *Plasmodium falciparum*-infected erythrocytes. Biochem. Pharmacol. 63, 393–398.

Genis, D., Kirpichenok, M., Kombarov, R., 2012. A minimalist fragment approach for the design of natural-product-like synthetic scaffolds. Drug Discov. today 17, 1170–1174.

Gong, P., Zhai, X., Liu, Y., Zhao, Y., Zhang, F., Jiang, N., 2013. Preparation of 4-aminoquinazoline derivatives as antitumor agents. Faming Zhuanli Shenqing.

Goodman, C.D., Su, V., McFadden, G.I., 2007. The effects of anti-bacterials on the malaria parasite *Plasmodium falciparum*. Mol. Biochem. Parasitol. 152, 181–191.

Greenwood, D., 1995. Conflicts of interest: the genesis of synthetic antimalarial agents in peace and war. J. Antimicrob. Chemother. 36, 857–872.

Gupta, P.B., Onder, T.T., Jiang, G., Tao, K., Kuperwasser, C., Weinberg, R.A., Lander, E.S., 2009. Identification of selective inhibitors of cancer stem cells by high-throughput screening. Cell 138, 645–659.

Hemphill, A., Mueller, J., Esposito, M., 2006. Nitazoxanide, a broad-spectrum thiazolide anti-infective agent for the treatment of gastrointestinal infections. Expert Opin. Pharmacother. 7, 953–964.

Howard, R.J., Miller, L.H., 1981. Invasion of erythrocytes by malaria merozoites: evidence for specific receptors involved in attachment and entry. Ciba Found. Symp. 80, 202–219.

Janiszewski, J.S., Rogers, K.J., Whalen, K.M., Cole, M.J., Liston, T.E., Duchoslav, E., Fouda, H.G., 2001. A high-capacity LC/MS system for the bioanalysis of samples generated from plate-based metabolic screening. Anal. Chem. 73, 1495–1501.

Johnson, J.D., Dennull, R.A., Gerena, L., Lopez-Sanchez, M., Roncal, N.E., Waters, N.C., 2007. Assessment and continued validation of the malaria SYBR green I-based fluorescence assay for use in malaria drug screening. Antimicrob. Agents Chemother. 51, 1926–1933.

Kansy, M., Senner, F., Gubernator, K., 1998. Physicochemical high throughput screening: parallel artificial membrane permeation assay in the description of passive absorption processes. J. Med. Chem. 41, 1007–1010.

Kombarov, R., Altieri, A., Genis, D., Kirpichenok, M., Kochubey, V., Rakitina, N., Titarenko, Z., 2010. BioCores: identification of a drug/natural product-based privileged structural motif for small-molecule lead discovery. Mol. Divers. 14, 193–200.

Krishna, S., Uhlemann, A.C., Haynes, R.K., 2004. Artemisinins: mechanisms of action and potential for resistance. Drug Resistance Updates Rev. Comment. Antimicrob. Anticancer Chemother. 7, 233–244.

Lambros, C., Vanderberg, J.P., 1979. Synchronization of *Plasmodium falciparum* erythrocytic stages in culture. J. Parasitol. 65, 418–420.

Lee, S., Lim, D., Lee, E., Lee, N., Lee, H.G., Cechetto, J., Liuzzi, M., Freitas-Junior, L.H., Song, J.S., Bae, M.A., Oh, S., Ayong, L., Park, S.B., 2014. Discovery of carbohybrid-based 2-aminopyrimidine analogues as a new class of rapid-acting antimalarial agents using image-based cytological profiling assay. J. Med. Chem. 57, 7425–7434.

Loria, P., Miller, S., Foley, M., Tilley, L., 1999. Inhibition of the peroxidative degradation of haem as the basis of action of chloroquine and other quinoline antimalarials. Biochem. J. 339, 363–370.

Margolis, B.J., Long, K.A., Laird, D.L.T., Ruble, J.C., Pulley, S.R., 2007. Assembly of 4-aminoquinolines via palladium catalysis: a mild and convenient alternative to SNAr methodology. J. Org. Chem. 72, 2232–2235.

Mattila, M.A., Larni, H.M., 1980. Flunitrazepam: a review of its pharmacological properties and therapeutic use. Drugs 20, 353–374.

Moon, S., Lee, S., Kim, H., Freitas-Junior, L.H., Kang, M., Ayong, L., Hansen, M.A., 2013. An image analysis algorithm for malaria parasite stage classification and viability quantification. PloS One 8, e61812.

Nallan, L., Bauer, K.D., Bendale, P., Rivas, K., Yokoyama, K., Horney, C.P., Pendyala, P.R., Floyd, D., Lombardo, L.J., Williams, D.K., Hamilton, A., Sebti, S., Windsor, W.T., Weber, P.C., Buckner, F.S., Chakrabarti, D., Gelb, M.H., Van Voorhis, W.C., 2005. Protein farnesyltransferase inhibitors exhibit potent antimalarial activity. J. Med. Chem. 48, 3704–3713.

Ncokazi, K.K., Egan, T.J., 2005. A colorimetric high-throughput beta-hematin inhibition screening assay for use in the search for antimalarial compounds. Anal. Biochem. 338, 306–319.

Neill, A.L., Hunt, N.H., 1992. Pathology of fatal and resolving Plasmodium berghei cerebral malaria in mice. Parasitology 105 (Pt 2), 165–175.

Pal, D., Banerjee, S., Cui, J., Schwartz, A., Ghosh, S.K., Samuelson, J., 2009. Giardia, Entamoeba, and Trichomonas enzymes activate metronidazole (nitroreductases) and inactivate metronidazole (nitroimidazole reductases). Antimicrob. Agents Chemother. 53, 458–464.

Peters, W., 1975. The chemotherapy of rodent malaria, XXII. The value of drug-resistant strains of *P. berghei* in screening for blood schizontocidal activity. Ann. Trop. Med. Parasitol. 69, 155–171.

Raether, W., Hanel, H., 2003. Nitroheterocyclic drugs with broad spectrum activity. Parasitol. Res. 90 (Suppl. 1), S19–S39.

Ribaut, C., Berry, A., Chevalley, S., Reybier, K., Morlais, I., Parzy, D., Nepveu, F., Benoit-Vical, F., Valentin, A., 2008. Concentration and purification by magnetic separation of the erythrocytic stages of all human Plasmodium species. Malar. J. 7, 45.

Rieckmann, K.H., 2006. The chequered history of malaria control: are new and better tools the ultimate answer? Ann. Trop. Med. Parasitol. 100, 647–662.

Rishton, G.M., 2008. Molecular diversity in the context of leadlikeness: compound properties that enable effective biochemical screening. Curr. Opin. Chem. Biol. 12, 340–351.

Roberts, B.F., Iyamu, I.D., Lee, S., Lee, E., Ayong, L., Kyle, D.E., Yuan, Y., Manetsch, R., Chakrabarti, D., 2016. Spirocyclic chromanes exhibit antiplasmodial activities and inhibit all intraerythrocytic life cycle stages. Int. J. Parasitol. Drugs Drug Resist 6, 85–92.

Saenz, F.E., Mutka, T., Udenze, K., Oduola, A.M., Kyle, D.E., 2012. Novel 4-aminoquinoline analogs highly active against the blood and sexual stages of Plasmodium in vivo and in vitro. Antimicrob. Agents Chemother. 56, 4685–4692.

Sandlin, R.D., Carter, M.D., Lee, P.J., Auschwitz, J.M., Leed, S.E., Johnson, J.D., Wright, D.W., 2011. Use of the NP-40 detergent-mediated assay in discovery of inhibitors of beta-hematin crystallization. Antimicrob. Agents Chemother. 55, 3363–3369.

Sanni, L.A., Fonseca, L.F., Langhorne, J., 2002. Mouse models for erythrocytic-stage malaria. Methods Mol. Med. 72, 57–76.

Singh, N.G.R., Giulianotti, M., Pinilla, C., Houghten, R., Medina-Franco, J.L., 2009. Chemoinformatic analysis of drugs, natural products, molecular libraries small molecule repository and combinatorial libraries. J. Chem. Inf. Model. 49, 1010–1024.

Sinha, M., Dola, V.R., Agarwal, P., Srivastava, K., Haq, W., Puri, S.K., Katti, S.B., 2014. Antiplasmodial activity of new 4-aminoquinoline derivatives against chloroquine resistant strain. Bioorg. Med. Chem. 22, 3573–3586.

Smilkstein, M., Sriwilaijaroen, N., Kelly, J.X., Wilairat, P., Riscoe, M., 2004. Simple and inexpensive fluorescence-based technique for high-throughput antimalarial drug screening. Antimicrob. Agents Chemother. 48, 1803–1806.

Sorkin, E.M., Clissold, S.P., Brogden, R.N., 1985. Nifedipine. A review of its pharmacodynamic and pharmacokinetic properties, and therapeutic efficacy, in ischaemic heart disease, hypertension and related cardiovascular disorders. Drugs 30, 182–274.

Srivastava, I.K., Rottenberg, H., Vaidya, A.B., 1997. Atovaquone, a broad spectrum antiparasitic drug, collapses mitochondrial membrane potential in a malarial parasite. J. Biol. Chem. 272, 3961–3966.

Thomas, K.D., Adhikari, A.V., Shetty, N.S., 2010. Design, synthesis and antimicrobial activities of some new quinoline derivatives carrying 1,2,3-triazole moiety. Eur. J. Med. Chem. 45, 3803–3810.

Trager, W., Jensen, J.B., 1976. Human malaria parasites in continuous culture. Science 193, 673–675.

Truong, D.D., 2009. Tolcapone: review of its pharmacology and use as adjunctive therapy in patients with Parkinson's disease. Clin. Interv. Aging 4, 109–113.

Tukulula, M., Njoroge, M., Abay, E.T., Mugumbate, G.C., Wiesner, L., Taylor, D., Gibhard, L., Norman, J., Swart, K.J., Gut, J., Rosenthal, P.J., Barteau, S., Streckfuss, J., Kameni-Tcheudji, J., Chibale, K., 2013. Synthesis and in vitro and in vivo pharmacological evaluation of new 4-aminoquinoline-based compounds. ACS Med. Chem. Lett. 4, 1198–1202.

Vasilevich, N.I., Kombarov, R.V., Genis, D.V., Kirpichenok, M.A., 2012. Lessons from natural products chemistry can offer novel approaches for synthetic chemistry in drug discovery. J. Med. Chem. 55, 7003–7009.

Walsh, J.S., Miwa, G.T., 2011. Bioactivation of drugs: risk and drug design. Annu. Rev. Pharmacol. Toxicol. 51, 145–167.

Wilkinson, S.R., Bot, C., Kelly, J.M., Hall, B.S., 2011. Trypanocidal activity of nitroaromatic prodrugs: current treatments and future perspectives. Curr. Top. Med. Chem. 11, 2072–2084.

Wilson, D.W., Langer, C., Goodman, C.D., McFadden, G.I., Beeson, J.G., 2013. Defining the timing of action of antimalarial drugs against *Plasmodium falciparum*. Antimicrob. Agents Chemother. 57, 1455–1467.

World Health Organization, 2016. World Malaria Report 2016. World Health Organization, Geneva, Switzerland.

Yan, Y., Xu, K., Fang, Y., Wang, Z., 2011. A catalyst-free benzylic C-H bond olefination of azaarenes for direct Mannich-like reactions. J. Org. Chem. 76, 6849–6855.